International Journal of Fluid Machinery and Systems
Vol. 2, No. 1, January-March 2009

Original Paper

Analysis of Aerodynamic Performance in an Annular Compressor Bowed Cascade with Large Camber Angles

Shaowen Chen and Fu Chen

School of Energy Science and Engineering
Harbin Institute of Technology
Harbin 150001 China

Abstract

The effects of positively bowed blade on the aerodynamic performance of annular compressor cascades with large camber angle were experimentally investigated under different incidences. The distributions of the exit total pressure loss and secondary flow vectors of compressor cascades were analyzed. The static pressure was measured by tapping on the cascade surfaces, and the ink-trace flow visualizations were conducted. The results show that the value of the optimum bowed angle and optimum bowed height decrease because of the increased losses at the mid-span with the increase of the caber angle. The C-shape static pressure distribution along the radial direction exists on the suction surface of the straight cascade with large r camber angles. When bowed blade is applied, the larger bowed angle and larger bowed height will further enhance the accumulation of the low-energy fluid at the mid-span, thus deteriorate the flow behavior. Under 60° camber angle, flow behavior near the end-wall region of some bowed cascades even deteriorates instead of improving because the blockage of the separated flow near the mid-span keeps the low-energy fluid near the end-walls from moving towards the mid-span region, and as a result, a rapid augmentation of the total loss is easy to take place under large bowed angle. With the increase of camber angle, the choice range of bowed angle corresponding to the best performance in different incidences become narrower.

Keywords: Cascade experiment, compressor, camber angle

1. Introduction

Improving the stage loading and the pressure ratio of the compressor system is one of the key technologies of the aero-engines with a thrust-weight ratio of 15–20 or higher. More heavily loaded blades should be developed to prevent the increase of the compressor stage because of the improvement of stage load and pressure ratio. Severe flow separations occurred as stage loading and turning angle increased, resulting in a rapid secondary flow loss augmentation. Bryce et al [1] and Emmerson [2] performed separately a dynamic test and a numerical research on some highly-loaded compressor. The results indicated that highly adverse pressure gradient took place in compressor cascades with large turning angles, which induced severe flow separations, and accordingly induced rapid loss augmentation and decrease of stage pressure ratio. Carter et al [3] tested the rectangular compressor cascade with a 69° camber angle, and the experimental results demonstrated that the compressor cascade with large turning angles had the characteristics of strong 3D separations and high aerodynamic losses. As an effective design way to restrain flow separations near the end-walls by controlling the 3D flow and to enhance efficiency and pressure ratio, bowed compressor blades have been widely recognized by the researchers from many countries. Wang et al [4, 5] believed that the flow losses and the crosswise secondary flow near the end-walls could be reduced with a positively bowed blade by controlling the radial and crosswise pressure gradient in compressor cascades, but the effects of a positively bowed blade on flow losses depended on the boundary layer separation degree and the axial pressure gradient on blade suction surface. Breugelmans et al [6] tested the rectangular compressor cascade with four stacking types, and the experimental results demonstrated that the end-walls flow should be improved by using the adaptive lean angle in bowed compressor cascades. Sasaki et al [7] tested the rectangular CDA compressor cascade with different positively bowed projects, and the experimental results showed that bowed angle and bowed height were not in direct proportion to performance improvement, and the performance parameters of the compressor cascade with a 15° bowed angle decreasing loss is optimal in all bowed projects. Wang et al [8] tested the annular bowed compressor cascades with a 59.5° camber angle and five different stacking types, and the result indicated that the positively bowed blade of a 25° bowed angle was the best type to decrease losses in design incidence. The researches above indicated, to a certain degree, that the

Received September 10 2008; revised November 17 2008; accepted for publication December 4 2008: Review conducted by Prof. Hideaki Tamaki (Paper number O08027)
Corresponding author: Chen Shaowen, Lecturer, cswemail@hit.edu.cn

improvements of the positively bowed blade on compressor aerodynamic performances were dependent on flow field characters. Although the positively bowed blade has been applied effectively in compressor cascades with a large turning angle, yet the researches on applying the positively bowed blade to compressor cascades with different camber angles and on analyzing flow situations and loss mechanism of large turning compressor cascades are still very few.

Three sets of bowed compressor cascades with a camber angle of 40°, 50° and 60° respectively were designed and investigated experimentally under different incidences in a low speed, large scale wind tunnel. Each set of the bowed cascades included one conventional straight blade cascade, three positive bowed blade cascades with a bowed angle of 15°, 20° and 25° respectively. At design condition, the detailed cascade flow fields and aero-dynamic parameters were measured, and the effects of positively bowed blade on aero-dynamic performance of compressor cascades with different camber angles were analyzed and discussed. Finally, the optimal area of bowed angles in compressor cascades with different camber angles was given at design condition.

2. Test facility and methods

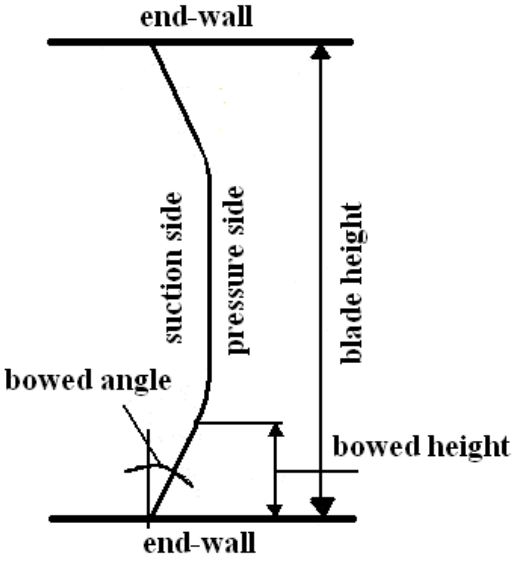

Fig.1 Definition of bowed blade stacking type

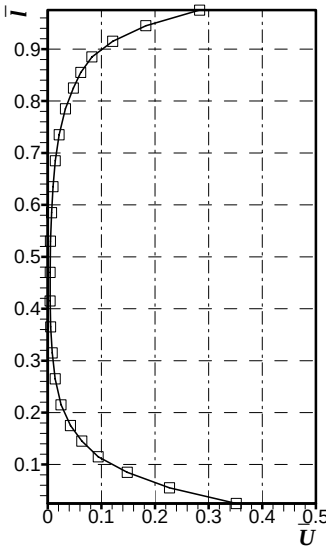

Fig.2 The behaviour of inlet boundary layer

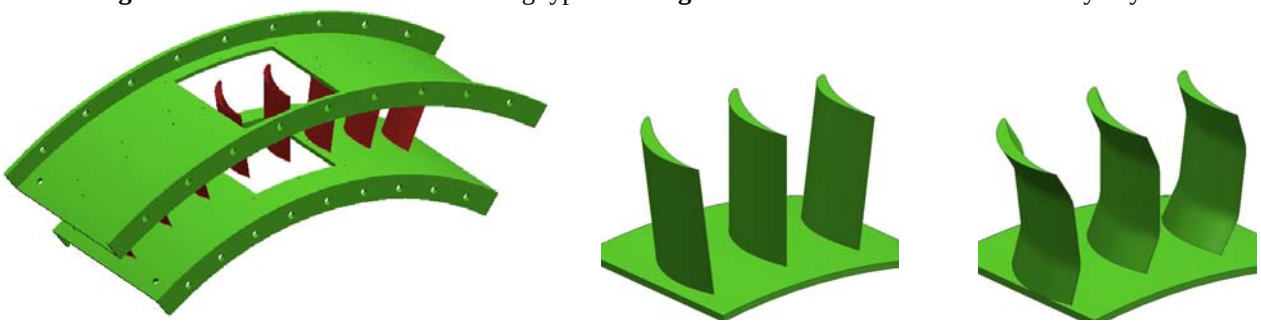

(a) tested cascades (b) straight blade(STR) (c)bowed blade(PB25)

Fig.3 Schematic diagram of tested annular compressor cascades

The tests were done in the low-speed annular cascade wind tunnel at the Institute of Propulsion Theory and Technology, Harbin Institute of Technology. It is a continuous flow facility without inlet boundary layer suction. A large centrifugal blower of 75KW forces air into the setting chamber, which is equipped with several different screens. The inlet velocity can be controlled by a valve. A five-hole was adopted to carry out the measurement, and was moved in spanwise and pitchwise directions by two step motors. The mechanical resolution of the device is about ±0.05mm for spanwise and ±0.1° for pitchwise movement. Pressure sensors PM10-1-2-S-0 and temperature sensors DBW-2-B were used with an accuracy of ±2%(-10℃~+50℃) and ±0.25°(-10℃~+50℃) respectively.

The positively bowed blade means an obtuse angle corner between end-wall and suction surface, while the negative bowed blade is an acute angle corner between. The bowed angle is the angle between the pressure side and the end-wall. The definition of the bowed angle and bowed height are shown in Fig. 1. The flow fields of three sets of bowed compressor cascades with a camber angle of 40°, 50° and 60° respectively were measured by “L” type five-hole probe in detail. Each set of bowed cascades included one conventional straight blade cascade (STR) and three positive bowed blade cascades with a bowed angle of 15° (PB15), 20° (PB20)and 25° (PB25) respectively. The schematic diagrams of tested annular compressor cascades and blades are shown in Fig. 3. Static pressure taps were installed on both the end-walls and blade surfaces to obtain the distribution of static pressure. The ink-trace flow visualizations were performed to show boundary layer development. The five-hole probe used in the experiment was calibrated separately in a low speed calibration tunnel at lower velocities for directional sensitivity whose yaw angle is ±30°. The

layout of measurement points in the radial and circumferential directions is 24×17. At any incidence, the experiments for all cascades were conducted with approximately the same inlet parameters. The inlet Mach number is about 0.23. The inlet Reynolds number is Re 5.27×10^5. The radius of the tip and the hub is 575mm and 475mm, respectively, and the aspect ratio is 1.0. The aerofoil used is the series of NACA65. The schematic of camber angles is shown in Fig. 4. The geometric and aerodynamic parameters of the cascades are shown in table 1 and the inlet boundary layer's behavior is shown in Fig.2.

Table 1 the geometric and aerodynamic parameters

Geometric parameters	
Camberangle(degree)	40, 50, 60
Bowed angle(degree)	0, 15, 20, 25
Bowed height	20%L
Chord(m)	0.1
Aspect ratio	1
Solidity	1.25
Stagger angle(degree)	10.39
Profile	NACA65-24A10-10
Aerodynamic parameters	
Turbulence (inlet)	5%
Re (inlet)	5.27×10^5
Incidence(degree)	-10, -5, 0, 5, 10

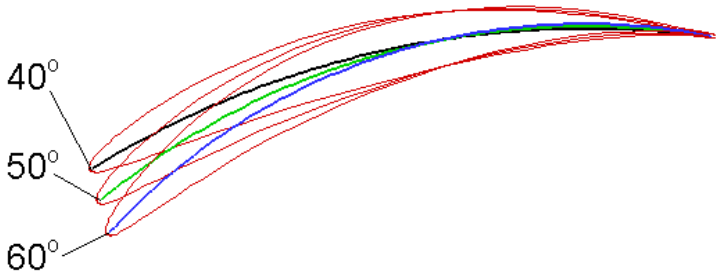

Fig.4 NACA65 blade aerofoil with three camber angles

3. Results and discussion

The distribution of pitch-mass-averaged total pressure loss coefficient along the blade height at the exit is given in Fig. 5. As seen from Fig. 5, the loss coefficient distribution along the blade height varies with the camber angle. The total pressure loss coefficient is defined as the difference between exit total pressure and inlet total pressure divided by inlet kinetic energy. Twenty-five percent of the axial chord downstream of the blade trailing edge is chosen as the location for comparison of exit properties. For convenience, 50%–100% of the blade height region is called "the upside", and 0%–50% of the blade height region is called the underside". The loss distributions in the upside and the underside of the cascade with a 40° camber angle are more symmetric than that with the camber angles of 50° and 60°. The minimum loss coefficient of the cascade with a 40° camber angle lies in the 50% blade height. The loss coefficient in the upside of the cascade with a 40° camber angle is higher than that in the underside of it, and the increase of loss coefficient lies mainly in the region of 60%–80% blade height. The minimum loss coefficient of the cascade with a 50° camber angle lies in the 40% blade height. The loss distributions in the upside and the underside of the cascade with a 60° camber angle are greatly asymmetric, and the loss in the upside of the cascade is lower than that in the underside of it. The minimum loss coefficient of the cascade with a 60° camber angle lies generally in 60% blade height, with the exception of the 50% blade height for straight cascade.

The effects on reducing the end-wall loss and increasing the middle loss by applying positively bowed blade in all cascades are also shown in Fig. 5. The effects of positively bowed blade on the exit loss along the blade height vary with the camber angle. The middle loss of positively bowed cascades increases with the augment of the camber angle, particularly distinct in the 25° positively bowed cascade with a 60° camber angle. There is a great change of the total pressure loss in the cascades with a camber angle of 40° and 60° at a blade height of 70%–80% by applying positively bowed blade, but the loss varieties are opposite. The total pressure loss increases in the cascades with 40° camber angle at a blade height of 70%–80%, and the loss increase reaches the maximum in the cascade of 15° positively bowed angle but it reaches the minimum in the cascade of 25° positively bowed angle. However, the total pressure loss decreases by using positively bowed blade in the cascades with a 60° camber angle at the blade height of 70%–80%, and the loss decrease reaches the maximum in the cascade with 15° positively bowed angle, but it reaches the minimum in the cascade with 25° positively bowed angle.

The effects of changed bowed angles on overall mass-averaged loss coefficient of the cascades with different camber angles are shown in Fig. 6. As the camber angles of cascades increase, the overall loss of cascades increases, and the loss increase reaches the minimum in the cascade with 15° positively bowed angle in all cascades, but opposite is true in the cascade of 25° positively bowed angle. The sharp augment of the middle loss leads to the sharp augment of total loss. Furthermore, there are different optimal bowed angles (the least total loss) in cascades with different camber angles.

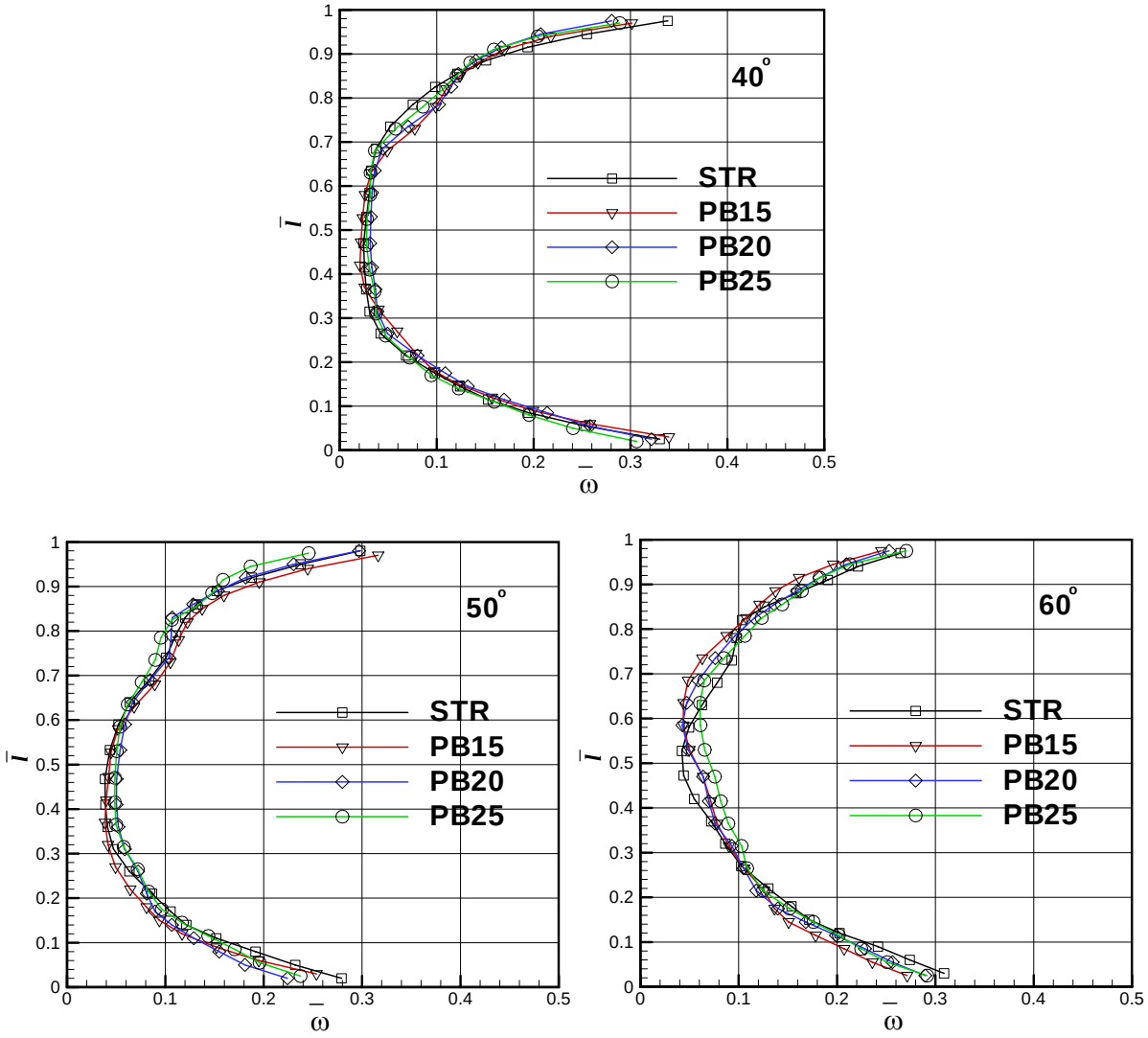

Fig.5 Distribution of pitch-mass-averaged total pressure loss coefficient along blade height (i=0°)

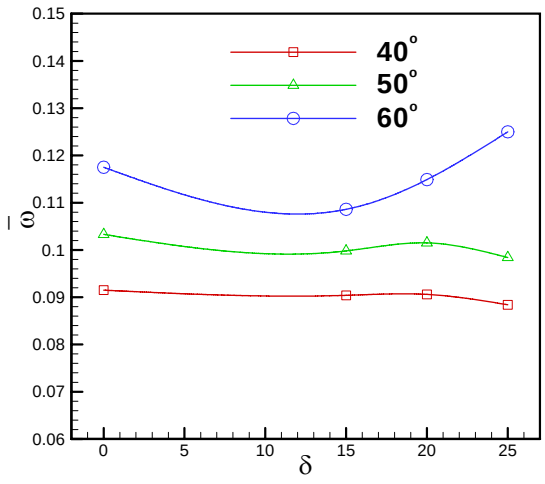

Fig.6 Effect of changed bowed angles on overall mass-averaged loss coefficient (i=0°)

Figure 7 demonstrates the contours of total pressure loss coefficients at cascade exit. As shown in Fig. 7, the total pressure loss concentrates near the end-walls and in the corner of the end-wall. Along with the augment of the camber angle, the loss near the corner of the end-wall increases. As a result of the radial pressure gradient from the tip to the hub in annular cascade, the low-energy fluid transits from the boundary layer at the mid-span and the tip to the hub. More low-energy fluid gathers at the hub with the increase of camber angle. The radial pressure gradient from the end-walls to the mid-span due to positively bowed blade makes the low-energy fluid at the corner transit to the mid-span. As shown in Fig. 7, the high loss core at the corners move to the mid-span in positively bowed cascades, and the moving increases with the augment of the camber angle. The high loss region at the corner of the end-wall dwindles in the positively bowed cascades significantly with a 60° camber angle but the loss at the mid-

span increases greatly, especially in the cascades with a 60° camber angle, which also can be seen in Fig. 5. Severe flow separation occurs as the camber angle increases, resulting in a rapid loss augmentation.

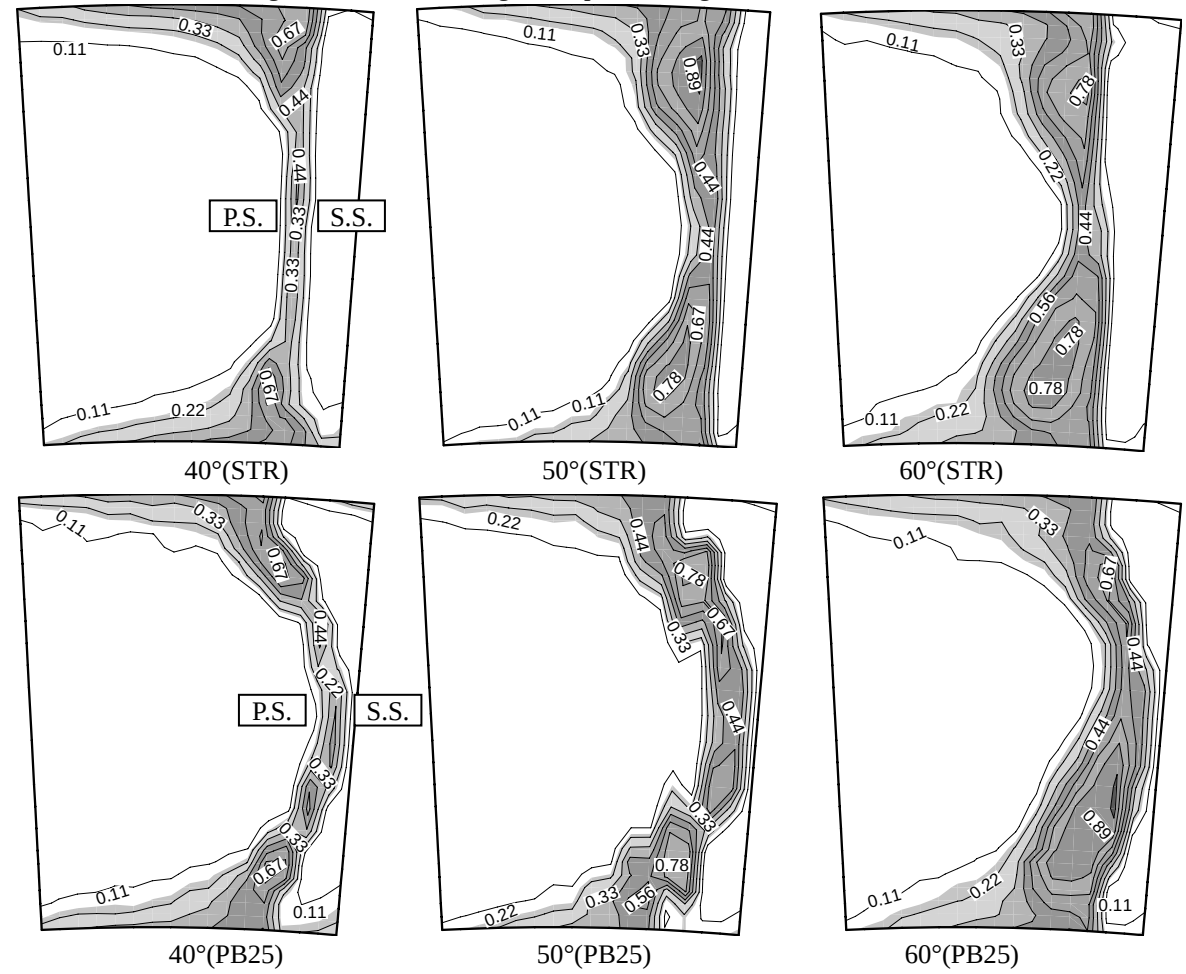

Fig. 7 Contours of total pressure loss coefficient at the cascade exit (i=0°)

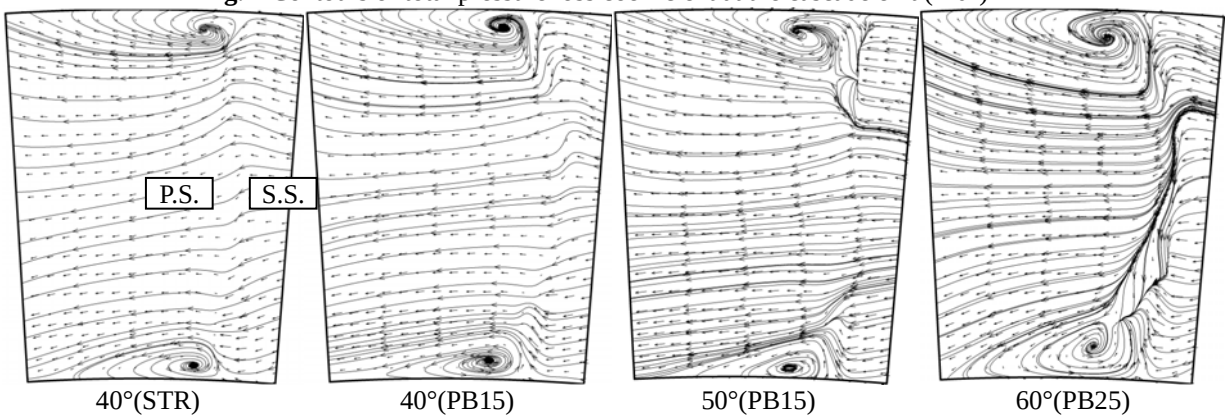

Fig. 8 Distribution of secondary flow vector at the cascade exit (i=0°)

Figure 8 demonstrates the distributions of the secondary flow vector and the limiting streamline at the cascade exit. Velocity vectors in the plane perpendicular to flow direction are the vectorial sums of *v* and *w*, and streamwise vorticity contours are obtained by finite differentiations of *v* and *w*. The range and intensity of the passage vortex increase and tend to extend to the mid-span and the pressure surface of the blade with the increase of the camber angle. With positively bowed blade, the passage vortex becomes stronger than the straight cascade at any camber angles, and the trend of low-energy flow transited to the mid-span is more obvious. With the increase of the camber angle, the severe separation enlarges to the whole blade height, resulting in a rapid loss augmentation.

The contours of static pressure coefficient and ink-trace flow visualization on suction surface are given separately in Fig. 9 and Fig. 10. As can be seen from Fig. 9, the C-shape static pressure distribution along the radial direction exists on the suction surface of the straight cascade with larger camber angles, which is beneficial to the movement of low-energy fluid from the end-wall corner to the mid-span. When bowed blade is applied, the larger bowed angle and larger bowed height will further enhance the accumulation of the low-energy fluid at the mid-span, thus deteriorating the flow behavior as shown in Fig. 10. The range of the flow separation the cascades with a 40° camber angle is the least of all cascades, and the effects of radial pressure gradient on low-energy fluid are slight. The flow separation regions at the end-walls in the cascades with 50° camber angle extend to the mid-span, and even to the whole blade height on suction surface with the application of 25° positively bowed blade. There is reverse flow at

the trailing edge of the mid-span. When camber angle is 60°, the flow separation on suction surface near the mid-span becomes stronger, and a vortex structure occurs in the mid-span, indicating that the larger camber angle, the stronger movement of low-energy fluid from the end-wall to the mid-span, leading to a severe flow separation and a rapid loss augmentation.

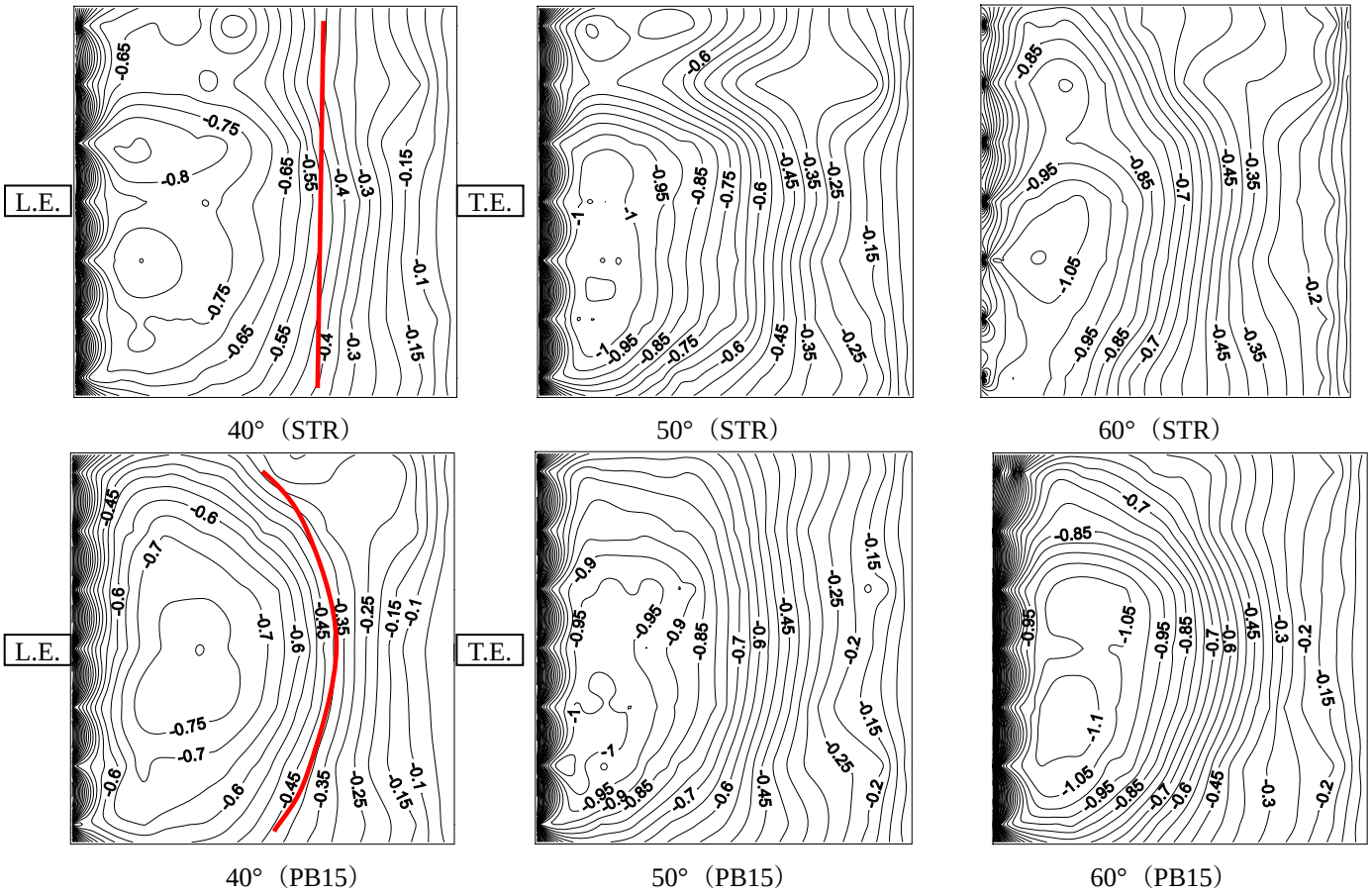

Fig. 9 Contours of static pressure coefficient on suction surface (i=0°)

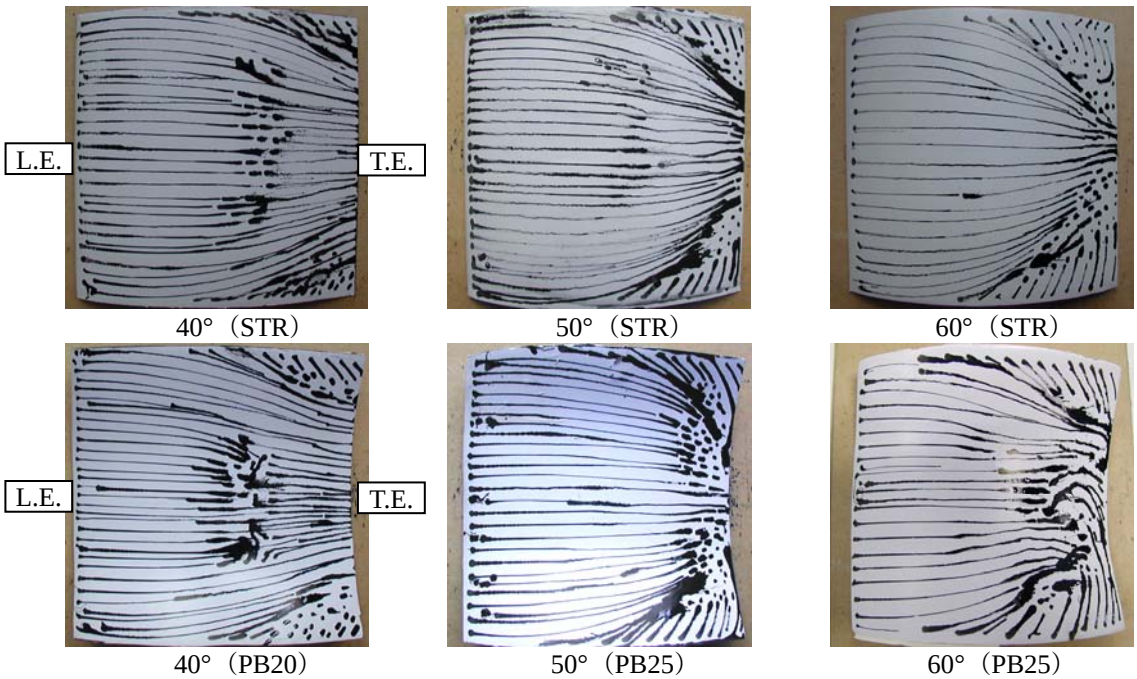

Fig. 10 Ink-trace flow visualization on suction surface (i=0°)

The distribution of pitch-mass-averaged exit flow angle along blade height with different camber angles is given in Fig. 11. The dash lines in the figure represent the geometric exit flow angle of the cascade. The exit flow angles at most blade heights are far away the geometry exit angles except near end-walls. There are the great underturnings of the flow at the mid-span of all cascades, and the slight underturnings or the approximate geometry exit angles occur at the two end-walls of most cascades, except that the slight overturnings are located at the hub of the cascades with 60° camber angle. With the augmentation of camber angle, the pitch-mass-averaged exit flow angles at 20%~80% relative blade height reduce gradually under 0° incidence, and the underturning

angles are larger, however, the great decrease of the pitch-mass-averaged exit flow angles are located at 50%–85% height of the cascades with 60° camber angle and 25° bowed angle under +5° incidence.

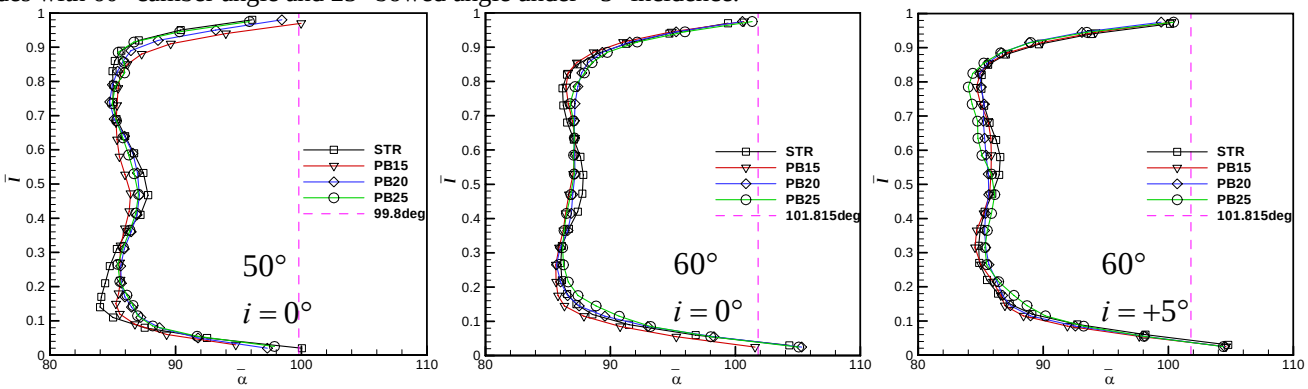

Fig.11 Distribution of pitch-mass-averaged exit flow angle along blade height

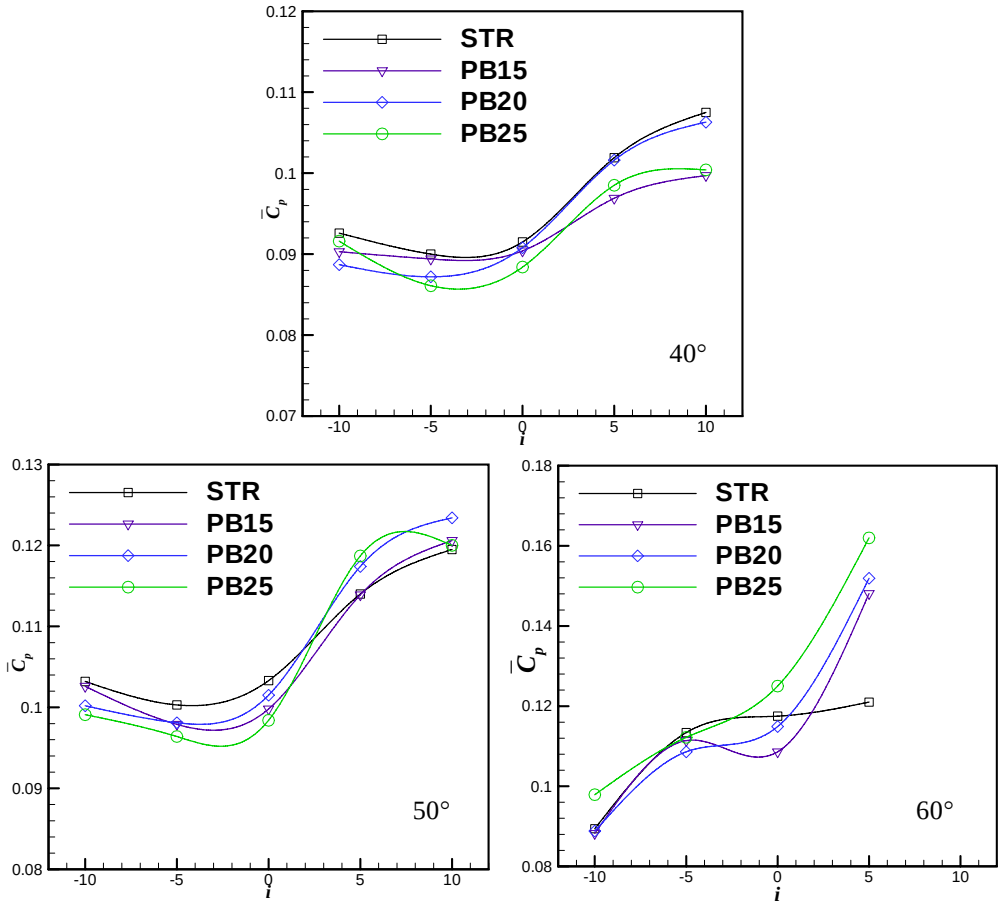

Fig.12 The mass averaged total pressure loss coefficient variation at exit with incidences

Incidence is one of the main factors which affect end secondary flow losses. As shown in Fig. 12, under the condition of 40° camber angle, the mass averaged total pressure loss coefficient of all positive bowed cascades is lower than that of straight cascades at any incidence. Under the condition of 50° camber angle, at 0° and negative incidence, the mass averaged total pressure loss coefficient of all positive bowed cascades is lower than that of straight cascades, but at positive incidences it is just opposite. Under the condition of 60° camber angle, at negative incidence, when positive bowed angle is small, the mass averaged total pressure loss coefficient is lower than that of straight cascades. At positive incidence, the total losses in positive bowed cascades are higher than that of straight cascades. The variety of losses is sensitive to incidences and bowed angles, so it needs cautious to apply positive bowed blade at high load.

4. Conclusion

With the increase of the camber angle, the value of the optimum bowed angle and optimum bowed height decreases due to the increased losses at the mid-span. The C-shape static pressure distribution along the radial direction exists on the suction surface of straight cascade with larger camber angles, which is beneficial to the movement of low-energy fluid from the end-wall to the mid-span. When bowed blade is applied, the larger bowed angle and larger bowed height will further enhance the accumulation of low-energy fluid at the mid-span, thus deteriorating the flow condition. The cascade of 60° camber angle and 25° bowed angle has a rapid total loss augmentation. With the increase of camber angle, the choice range of bowed angle corresponding to the best performance in different incidences become narrower. The effects of incidence angles on the aerodynamic performance of positive bowed cascade with large camber angle are more evident contrast to with small camber angle. The performance of

positive bowed cascade with 60°camber angle is so sensitive to the bowed angle changing at higher incidence angle, the positive bowed cascade with larger bowed angles than 15°is inadvisable.

Acknowledgments

The authors would like to acknowledge the support of National Natural Science Foundation of China, Grant No.50236020

Nomenclature

ω	Mass-averaged total pressure loss coefficient	C_p	Pitch-averaged total pressure loss coefficient
L	Length of blade[m]	δ	Bowed angle [^{o}]
i	Incidence angle [^{o}]	*L.E.*	Leading edge
T.E.	Trailing edge	*P.S.*	Pressure side
S.S.	Suction side		

References

[1] Bryce, H. D., Cherrett, M. A., Lyes, P. A., 1995, Three-dimensional flow in a highly loaded single-stage transonic fan," ASME Journal of Turbomachinery, Vol. 117, No. 2, pp. 22-25.
[2] Emmerson, P. R., 1996, Three-dimensional flow calculations of the stator in a highly loaded transonic fan,"ASME Turbo Expo, Amsterdam, Birmingham , 96-GT-546.
[3] Carter, C. J., Guillot, S. A., Ng, W. F., 2001, Aerodynamic performance of a high-turning compressor stator with flow control, AIAA Paper, 2001-3973.
[4] WANG, Z. Q., SU, J. X., ZHONG, J. J., 1994, New progress of investigation into mechanism of reducing energy loss in cascades with curved and twisted blades, Journal of Engineering Thermophysics, 15(2): 40-44 (in Chinese)
[5] Wang, H. S., Zhong, J. J., 2002, Wang, Z. Q., Effects of blade positive curving on aerodynamic performance of compressor cascades, Journal of Propulsion Technology, Vol. 23, No. 4, pp. 321-324.
[6] Breugelmans, F. A. E., 1985, Influence of incidence angle on the secondary flow in compressor cascade with different dihedral distribution, Beijing, ISABE Paper 85-7078.
[7] Sasaki, T., Breugelmans, F. A. E., 1998, Comparison of sweep and dihedral effects on compressor cascade performance, Transactions of ASME Journal of Turbormachinary, Vol. 120, No. 4, pp. 454-463.
[8] Wang, D., 2001, Experimental investigations of blade curving effect on aerodynamic characteristics of compressor cascades, Ph. D. Thesis, Department of Energy Science and engineering, Harbin Institute of Technology, Harbin, China.